Hypertension Research (2016) 39, 302–311

www.nature.com/hr

ORIGINAL ARTICLE

Reversal of right ventricular remodeling by dichloroacetate is related to inhibition of mitochondria-dependent apoptosis

Xiao-Qing Sun[1], Rui Zhang[1], Hong-Da Zhang[1], Ping Yuan[1], Xiao-Jian Wang[2], Qin-Hua Zhao[1], Lan Wang[1], Rong Jiang[1], Harm Jan Bogaard[3] and Zhi-Cheng Jing[1,2]

Most patients with pulmonary arterial hypertension die from right ventricular failure (RVF). Right ventricular (RV) myocardial apoptosis has an important role in RVF and is regulated by the mitochondria. Dichloroacetate (DCA) can improve cardiac function in RVF, but whether it can regulate myocardial apoptosis via mitochondria is still unknown. In this study, we investigated the effects of DCA on myocardial mitochondria, the mitochondrial apoptosis and other aspects of RV remodeling, including fibrosis and capillary rarefaction. RVF was induced in rats by a single s.c. injection of monocrotaline. After 4 weeks, DCA treatment was started with i.p. injection of 50, 150 or 2007 mg kg^{-1} per day during 14 days. Compared with saline-treated RVF animals, treatment with DCA resulted in decreased mean pulmonary arterial pressure and total pulmonary resistance (TPR), and increased cardiac output. The expression of pyruvate dehydrogenase kinase was suppressed, while pyruvate dehydrogenase expression was upregulated with DCA application. DCA treatment was also associated with restored RV mitochondrial function and a reduction in RV hypertrophy, fibrosis, capillary rarefaction and apoptosis. Mitochondria-dependent apoptosis was involved in DCA regulation of RV. The absent correlation between TPR and main parameters in RV suggests that the effects of DCA in the two organ systems are independent. We conclude that DCA improves cardiac function in experimental RVF partly by reversing RV remodeling, restoring mitochondrial function and regulating mitochondria-dependent apoptosis. The study shows that a fear for increased RV apoptosis with DCA treatment is unnecessary and suggests a potential role of DCA in the treatment of RVF.
Hypertension Research (2016) **39,** 302–311; doi:10.1038/hr.2015.153; published online 14 January 2016

Keywords: apoptosis; mitochondria; pulmonary arterial hypertension; right ventricular failure; right ventricular remodeling

INTRODUCTION

Pulmonary arterial hypertension (PAH) is a fatal disease characterized by pulmonary vascular remodeling and a chronically and frequently progressive increase in right ventricle (RV) afterload, causing RV remodeling and right ventricular failure (RVF).[1] Although the initial insult in PAH involves the pulmonary vasculature, RVF is the most important determinant of longevity in patients with PAH.[2] Recent animal data suggest that RV remodeling contributes to the progression of RVF.[3] Many questions, however, regarding the mechanisms underlying RV remodeling remain unanswered. Abnormal RV remodeling may be amenable to therapeutic intervention.

It has become clear that myocardial apoptosis is involved in RV remodeling and has an important role in RVF.[4] While inhibition of myocardial apoptosis is a viable therapeutic strategy for left ventricular (LV) failure,[5] recent studies indicate that suppressing apoptosis can also be beneficial in experimental RVF.[6,7] Therefore, reducing myocardial apoptosis may provide a new therapeutic strategy in patients with RVF. Meanwhile, it now becomes clear that mitochondria act to integrate diverse proapoptotic stimuli by releasing apoptosis-promoting factors such as cytochrome *c*, Smac/Diablo and the flavoprotein AIF.[8] Given the known role of mitochondria as apoptotic controllers, it is tempting to speculate that therapies targeting mitochondria can regulate RV myocardial apoptosis and improve RV function.

Mitochondrial abnormalities are not only closely related to induction of apoptosis but also to deregulated metabolism.[9–11] Indeed in RVF, myocardial apoptosis occurs alongside several metabolic changes and may be linked on the level of the mitochondria. Metabolic changes in RVF include increased activity and expression of pyruvate dehydrogenase kinase (PDK), which causes phosphorylation and inhibition of pyruvate dehydrogenase (PDH). PDH phosphorylation inhibits formation of acetyl-CoA and therefore slows the Krebs' cycle,

[1]Department of Cardio-Pulmonary Circulation, Shanghai Pulmonary Hospital, Tongji University School of Medicine, Shanghai, China; [2]State Key Laboratory of Cardiovascular Disease, Fu Wai Hospital, National Center for Cardiovascular Disease, Peking Union Medical College and Chinese Academy Medical Science, Beijing, China and [3]Department of Pulmonary Medicine, VU University Medical Center, Amsterdam, The Netherlands
Correspondence: Professor Z-C Jing, State Key Laboratory of Cardiovascular Disease, Fu Wai Hospital, National Center for Cardiovascular Disease, Peking Union Medical College and Chinese Academy Medical Science, Beijing, China.
E-mail: jingzhicheng@vip.163.com
Received 8 July 2015; revised 7 November 2015; accepted 30 November 2015; published online 14 January 2016

causing an increase in glycolysis relative to glucose oxidation.[12] Even though during short-term stress this metabolic switch seems beneficial, long-term reliance on glycolysis for ATP generation appears insufficient and contributes to the development of RVF.[13] Dichloroacetate (DCA) is a small molecular inhibitor of all four PDK isoforms and has shown promise as a new therapy for RVF.[14,15] By reducing PDH phosphorylation and improving glucose oxidation, DCA improved cardiac output (CO) in animal models of RVF.[9,16]

Because DCA not only reverses metabolic derangements but also effectively targets mitochondrial related pathways of apoptosis,[8,17] at least some of DCA's beneficial effects in RVF may come about through modulation of myocardial apoptosis. However, the effect of DCA on RV myocardial apoptosis is not clear. And previous studies on DCA and apoptosis seem inconsistent. A study on pulmonary vasculature suggests that DCA increases mitochondria-dependent apoptosis in pulmonary arterial smooth muscle cell in PAH.[17] Thus, it is possible that DCA would also promote RV apoptosis in PAH-induced RVF, which would largely limit the application of DCA in PAH. However, an *in vitro* study showed that DCA prevented H_2O_2-induced cell apoptosis in cultured cardiomyocytes.[18] To support DCA treatment on PAH, it is of great importance to figure out the effect of DCA on myocardial apoptosis in RVF *in vivo*. Moreover, recent data show that the development of RVF is also associated with multiple maladaptive RV remodeling including fibrosis, and a decreased RV capillary density,[3] but whether DCA can have an effect on these aspects of experimental RV remodeling is still unknown.

Here we hypothesize that DCA improves cardiac function in PAH-induced RVF through a mechanism involving modulation of RV mitochondrial function and mitochondria-dependent apoptosis. Thus, we sought to discover the possible mechanisms underlying the effects of DCA on RVF by (1) evaluating the effects of DCA on RV remodeling including myocardial apoptosis, fibrosis and capillary rarefaction, (2) examining the effects of DCA on mitochondrial structure and function and (3) assessing the mitochondria-dependent apoptotic pathway in RVF by application of DCA.

METHODS

Monocrotaline rat model of RVF

A total of 60 adult male Sprague–Dawley rats (from the Second Military Medical University Affiliated Experimental Animal Center; body weights 250–300 g) were divided into two groups: rats received a single s.c. injection of saline (control, $n=10$) or monocrotaline (MCT, 60 mg kg^{-1}; Sigma-Aldrich, St Louis, MO, USA) to induce RVF ($n=50$).[19] To determine the effects of different DCA doses on the progression of established RVF, 4 weeks later rats with induced RVF were randomly divided into four groups: rats with a daily i.p. injection of saline (MCT-induced RVF (MCT-RVF), $n=14$) or, respectively, 50, 150 or 200 mg kg^{-1} ($n=12$) DCA (Sigma-Aldrich) during 14 days. Later, rats were anesthetized for hemodynamic assessment and RV tissues were separated for further measurements.

All experimental procedures involving animals were executed conforming to the US National Institute of Health regulations and were approved by the Institutional Committee for Use and Care of Laboratory Animals of Tongji University.

Hemodynamic evaluation

Six weeks after receiving a single s.c. injection of saline or MCT, all surviving rats (control, 100% survival rate; MCT-RVF, 50% survival rate; DCA 50 mg kg^{-1}, 67% survival rate; DCA 150 mg kg^{-1}, 75% survival rate; DCA 200 mg kg^{-1}, 75% survival rate) were anesthetized with an i.p. injection of i.p. sodium pentobarbital (40 mg kg^{-1}), and hemodynamic parameters were measured by a polygraph system (PowerLab 8/30; ADInstruments, Bella Vista, NSW, Australia). Adequate anesthesia was monitored by determining the withdrawal response to a paw pinch and respiration monitoring. After tracheotomy, a polyethylene-50 catheter was inserted via the right external jugular vein into the pulmonary artery to assess mean pulmonary arterial pressure (mPAP) and CO. With these values the total pulmonary resistance (TPR = mPAP/CO) was calculated.

Assessment of RV hypertrophy index

After assessing hemodynamic parameters, the animals were killed by removal of the heart under deep anesthesia. After the atria, the pulmonary trunk and the aorta were removed from the excised heart, the RV wall was separated from the LV wall and ventricular septum. Wet weights of the RV, free LV and ventricular septum were determined. The ratio of RV weight to LV plus septum weight (RV(LV+S)) was calculated for assessment of RV hypertrophy.[19,20]

Histology, TUNEL and DNA laddering

For analysis of RV dimensions, hearts were fixed *in situ*, embedded in paraffin and stained with hematoxylin and eosin, as described previously.[21] Masson's Trichrome stain was used to assess the degree of fibrosis in cardiac sections. Fibrosis was quantified on digitized images, on which blue-stained tissue areas are expressed as percentage of the total surface area.[7] A mean cardiomyocyte cross-sectional area was determined in RV cryosections stained with hematoxylin and eosin and the capillary density was determined by isolectin B4 (Vector, Burlingame, CA, USA) staining.[21] Apoptotic cells were assessed by the terminal-deoxynucleotidyltransferase-mediated 2′-deoxyuridine 5′-triphosphated nick-end-labeling (TUNEL) method (EMD Millipore, Billerica, MA, USA). Using a magnification rate of 400, the percentages of TUNEL-positive cells were calculated in 10 randomly chosen fields of each section from three animals per group. The procedures of DNA laddering were exactly as described previously.[22]

Transmission electron microscopy

The ultrastructure of mitochondria was analyzed using transmission electron microscopy, as described previously.[10] Briefly, resuspended EV pellet (3 μl) was fixed with 2.5% glutaraldehyde, postfixed in buffered 1% OsO_4 with 1.5% $K_4Fe(CN)_6$, embedded in 1% agar and processed according to standard Epon812 embedding procedure. Mitochondria were visualized on thin sections (60 nm) with a transmission electron microscope (JEM1230, Tokyo, Japan) at 80 kV.

Real-time quantitative reverse transcription-polymerase chain reaction

Total RNA was isolated from the tissues of three rats per group using Trizol reagent according to the manufacturer's protocol. RNA concentration and purity were measured with a spectrophotometer at A260 and A260/280, respectively. The reverse transcription reaction was performed with the Gene Amp PCR System 9700 (Applied Biosystems, Carlsbad, CA, USA) for the first-strand cDNA synthesis. Reverse transcription-polymerase chain reaction was performed on an ABI 7500 apparatus (ABI, New York, NY, USA). The sequences of primers used were as follows: lactate dehydrogenase (LDHA), forward: 5′-CAAACTGCTCATCGTCTCAAAC-3′ and reverse: 5′-GCAACCAC TTCCAATAACTCTGT-3′; superoxide dismutase 2 (SOD2), forward: 5′-GGCT TCAATAAGGAGCAAGGT-3′ and reverse: 5′-TCTCCCAGTTGATTACATT CCA-3′; glyceraldehyde-3-phosphate dehydrogenase (GAPDH), forward: 5′-AC AGCAACAGGGTGGTGGAC-3′ and reverse: 5′-TTTGAGGGTGCAGCGAA CTT-3′. The PCR conditions were as follows: a predenaturing at 95 °C for 30 s, followed by 40 cycles of denaturation at 95 °C for 5 s, and annealing/extension at 60 °C for 34 s. A relative amount for each gene examined was obtained from a standard curve generated by plotting the cycle threshold value against the concentration of a serially diluted RNA sample expressing the gene of interest. This amount was normalized to the level of GAPDH mRNA.

Western blotting

Western blotting was performed using RV lysates from three rats per group. The protein concentration was determined by Pierce BCA Protein Assay Kit (Thermo Fisher, Waltham, MA, USA) with bovine serum albumin as the standard. Polyvinylidence fluoride membranes were probed by mouse monoclonal GAPDH (1:8000), rabbit monoclonal PDHα1 (1:1000), rabbit polyclonal Bax (1:1000), Bcl-2 (1:1000), LDHA (1:1000) and cleaved caspase-9 (1:1000)

from Cell Signaling Technology (Beverly, MA, USA); rabbit monoclonal PDK2 (1:500) and polyclonal active caspase-3 (1:200), mouse monoclonal SOD2 (1:2000; Abcam, Cambridge, UK); rabbit polyclonal PDK4 (1:1000; Sigma-Aldrich, Poole, UK) and goat polyclonal PDHα2 (1:200; Santa Cruz Biotechnology, Dallas, TX, USA) antibodies overnight with constant shaking at 4 °C. After washing three times for 10 min in TBS-T buffer, membranes were incubated with an appropriate horseradish peroxidase-conjugated antibody and enhanced chemiluminescence reagent (Thermo Fisher, Waltham, MA, USA). Band intensities were determined using Quantity One software from Bio-Rad (Hercules, CA, USA). All measurements were replicated at least three times.

Measurements of mitochondrial cytochrome *c* release into cytosol

Measurements of cytosolic cytochrome *c* were achieved by subcellular fractionation and western blotting with cytochrome *c* antibody (1:1000; Cell Signaling Technology) as described previously.[23] The purity of the cytosolic fractions was validated by western blotting using antibodies to cytochrome *c* oxidase subunit IV (1:1000; Cell Signaling Technology).

Statistical analysis

Data were presented as mean ± s.d. and were analyzed using one-way analysis of variance with Bonferroni *post hoc* comparisons. Correlations between TPR and RV parameters were calculated using Spearman's correlation coefficients. A *P*-value <0.05 was accepted as an indication of statistical significance. All statistical computations were performed using the Statistical Package for the Social Sciences version 13.0 software (SPSS, Chicago, IL, USA).

RESULTS

DCA improved hemodynamic parameters in MCT-RVF rats

After 2 weeks of treatment with DCA, there was no evident difference in the body weight between the MCT-RVF group and the DCA groups, or between the three DCA treatment groups of different dosages. Rats challenged with MCT consistently developed significant PAH, with higher mPAP and TPR, and lower CO. DCA treatment resulted in a marked reduction in mPAP by 29%, 32% and 36% after application of, respectively, 50, 150 and 200 mg kg^{-1} (Figure 1a). CO was reduced in the MCT group compared with the control group (81 ± 6.3 *vs.* 184 ± 11.5, $P<0.001$; Figure 1b) and DCA improved CO by 45%, 65% and 78% in MCT-RVF rats after application of, respectively, 50, 150 and 200 mg kg^{-1} (Figure 1b). In addition, treatment with DCA 50, 150 and 200 mg kg^{-1} resulted in a marked reduction in TPR by, respectively, 52%, 57% and 58% (Figure 1c), and no significant differences were found between the treatment groups.

DCA reversed RV remodeling in RVF

As shown by the ratio of RV weight to LV plus septum weight (RV/(LV+S)), there was significantly less hypertrophy in DCA-treated animals than in saline-treated MCT animals (Figure 1d). To further evaluate the effect of DCA treatment on RV remodeling, we performed a morphometric analysis of RV myocytes cardiomyocyte cross-sectional area, RV fibrosis, capillary density and myocardial apoptosis in these five groups of rats. DCA treatment significantly reduced RV cardiomyocyte cross-sectional area that was otherwise enlarged in MCT rats (Figures 2a and d). Moreover, RVF resulted in a loss of RV capillaries (Figures 2b and e). In contrast, DCA treatment partly recovered the normal density of RV capillaries (Figures 2b and e). Additionally, the RV of MCT rats developed a high degree of fibrosis, and DCA treatment markedly reduced the overall fibrosis in RV (Figures 2c and f).

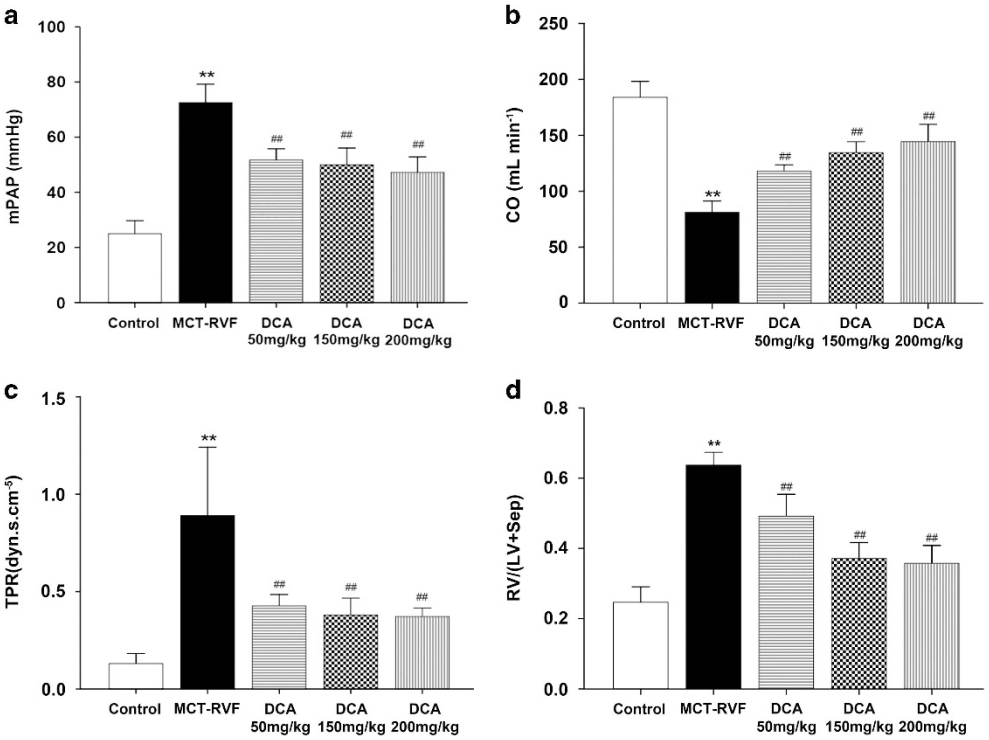

Figure 1 DCA improves hemodynamics and cardiac function in monocrotaline-induced right ventricular failure (MCT-RVF). (**a**) Mean pulmonary artery pressure (mPAP); (**b**) cardiac output (CO); (**c**) total pulmonary resistance (TPR); and (**d**) the ratio of free wall of RV weight to LV+Sep weight. Data shown are means ± s.d. of 7–10 rats per group. $^{**}P<0.001$: compared with the control group; $^{\#\#}P<0.001$: compared with the MCT-RVF group. DCA 50 mg kg^{-1}, DCA 50 mg kg^{-1} per day group; DCA 150 mg kg^{-1}, DCA 150 mg kg^{-1} per day group; DCA 200 mg kg^{-1}, DCA 200 mg kg^{-1} per day group; LC, left ventricular; Sep, septum.

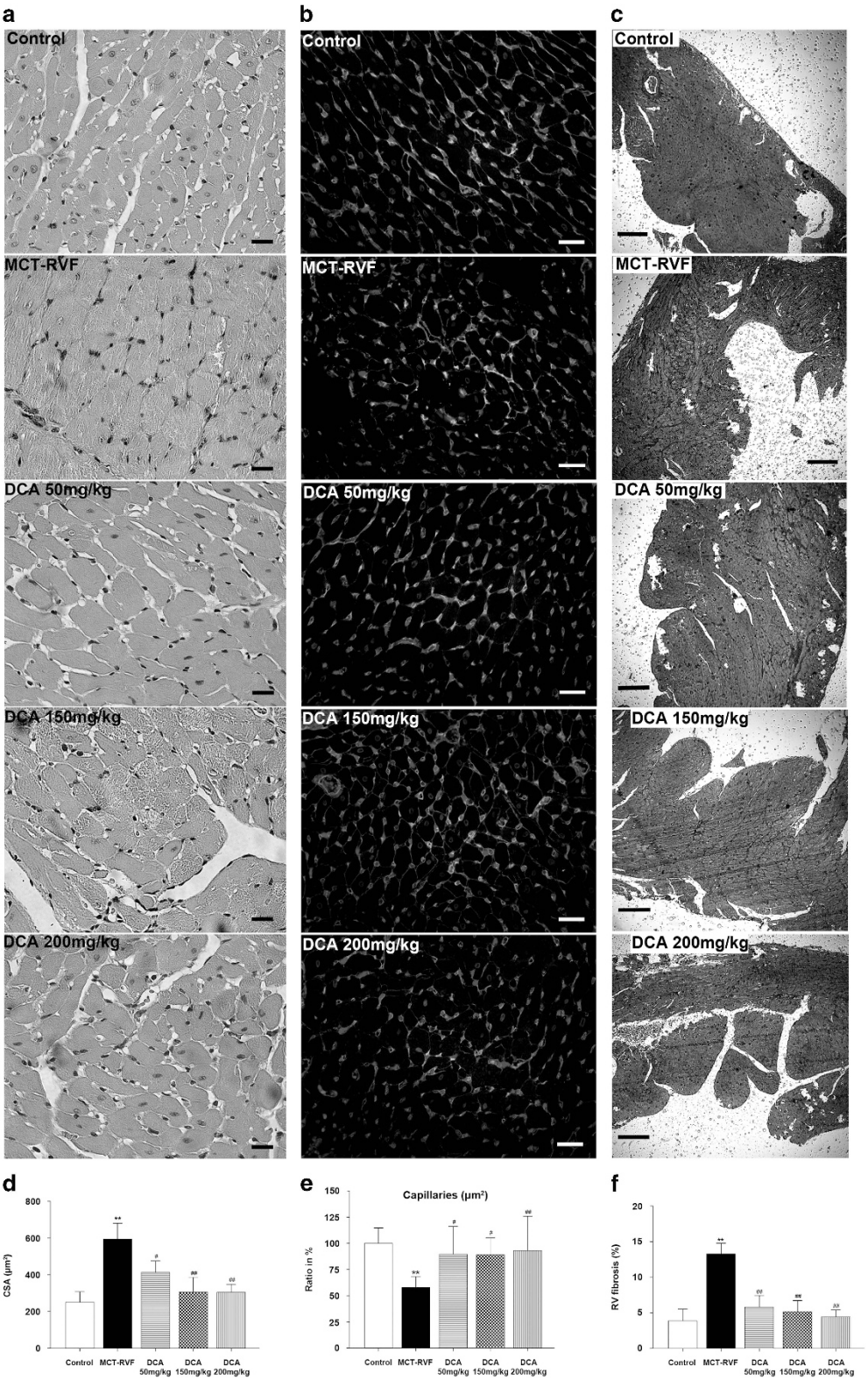

Figure 2 Dichloroacetate (DCA) partly reversed right ventricular (RV) remodeling in RV failure (RVF). (**a**) Hematoxylin and eosin staining of *in situ* fixed RV sections; scale bar = 20 μm. (**b**) RV cryosections stained with isolectin B4 (blood vessels, red), WGA (wheat germ agglutinin; cell membranes, green) and nuclei (4',6-diamidino-2-phenylindole; DAPI, blue), scale bar: 20 μm. (**c**) Fibrotic areas are shown by Masson trichrome stain, scale bar: 100 μm. (**d**) Quantitative analysis of mean cross-sectional area (CSA) of RV cardiomyocytes. (**e**) Capillaries to area (μm^2) ratio. (**f**) Fibrosis quantification (blue-stained areas expressed as the percentage of total RV surface area) of digitized images. $^{*}P<0.05$, $^{**}P<0.001$: compared with the control group; $^{\#}P<0.05$, $^{\#\#}P<0.001$: compared with the monocrotaline-induced right ventricular failure group (MCT-RVF) group. DCA 50 mg kg^{-1}, DCA 50 mg kg^{-1} per day group; DCA 150 mg kg^{-1}, DCA 150 mg kg^{-1} per day group; DCA 200 mg kg^{-1}, DCA 200 mg kg^{-1} per day group. A full color version of this figure is available at the *Hypertension Research* journal online.

DCA inhibited RV myocardial apoptosis in RVF

To determine whether DCA can reverse RV remodeling by inhibiting apoptosis in RV myocytes, TUNEL staining and DNA laddering were used. The percentage of TUNEL-positive nuclei was significantly greater in the MCT-RVF group (Figure 3b) compared with the control group (Figure 3a), and DCA treatment reduced the TUNEL-positive nuclei percentage (Figures 3c and f). Moreover, a weak pattern of DNA laddering was observed in both the control and DCA groups, but a much stronger DNA laddering pattern was found in the MCT-RVF group (Figure 3g).

DCA improved RV myocardial mitochondrial function in RVF

Transmission electron microscopy of the RV cardiomyocytes demonstrated that the mitochondrial ultrastructure in MCT-RVF tissues was highly abnormal, including swelling and a decreased number of mitochondria (Figure 4a). Moreover, in comparison with the controls, MCT-RVF tissues revealed medullary sheath-like degeneration, dissolution of the myofilaments, broken Z-lines and an irregular pattern of transverse striations (Figure 4a). Although these abnormalities were also present in the DCA 50 mg kg^{-1} treatment group, the defects in mitochondrial shape, size and number were obviously alleviated in the DCA 150 and 200 mg kg^{-1} treatment groups (Figure 4a).

Western blotting results demonstrated that both PDK2 and PDK4 proteins were upregulated in MCT-RVF rats. DCA reduced the protein expression of PDK2 and PDK4 (Figures 4c and f). However, the protein expression of PDK1 was unaltered in MCT-RVF rats, and DCA had no effect on PDK1 expression (Figures 4c and f). Accordingly, both PDHα1 and PDHα2 protein expression, which were depressed in the MCT-RVF group, were increased by DCA treatment (Figures 4c and f).

To further determine the effects of DCA on mitochondrial function, leakage of cytochrome *c* from mitochondria, SOD2 and LDHA expression were examined. The absence of cytochrome *c* oxidase subunit IV in the cytosolic fractions confirmed that the cytosolic preparations were free of mitochondrial contamination. Compared with the control group, leakage of the cytochrome *c* from the mitochondria to the cytosol increased in MCT rats (Figures 4e and g). DCA treatment decreased the leakage of cytochrome *c* from the mitochondria in RV cardiomyocytes when applied at a dose of 50, 150 and 200 mg kg^{-1} per day for 2 weeks (Figures 4e and g). Moreover, the gene expression of SOD2 in RV from saline MCT rats was significantly lower compared with that from the control group (Figure 4b), and was increased toward normal in all three DCA treatment groups (Figure 4b). Consistently, the SOD2 protein expression was also decreased in the MCT group and increased in the DCA groups (Figures 4d and g). Additionally, while LDHA gene expression was upregulated in MCT rats compared with the control group, the upregulation was suppressed in both the DCA 150 and 200 mg kg^{-1} groups (Figure 4b). Accordingly, western blotting showed that its protein expression was also markedly increased in the MCT group and decreased in the DCA treatment groups with doses of 150 or 200 mg kg^{-1} (Figures 4d and g).

DCA reduced RV cardiomyocytes apoptosis by regulating the mitochondria-dependent apoptotic pathway

As shown by TUNEL staining and DNA laddering, RV myocardial apoptosis increased in the MCT-RVF, while it was suppressed by DCA treatment (Figures 3f and g). Furthermore, to determine whether mitochondria-dependent apoptosis was involved, we detected the critical proteins by western blotting.

As Bcl-2 family member proteins mediate the mitochondrial apoptotic pathway, we examined the effect of DCA on Bcl-2 and Bax expression (Figure 5a). The expression of Bcl-2 protein was repressed in the MCT-RVF group compared with the control group, whereas DCA 150 and 200 mg kg^{-1} significantly upregulated Bcl-2 protein expression (Figures 5a and b). In contrast, Bax protein

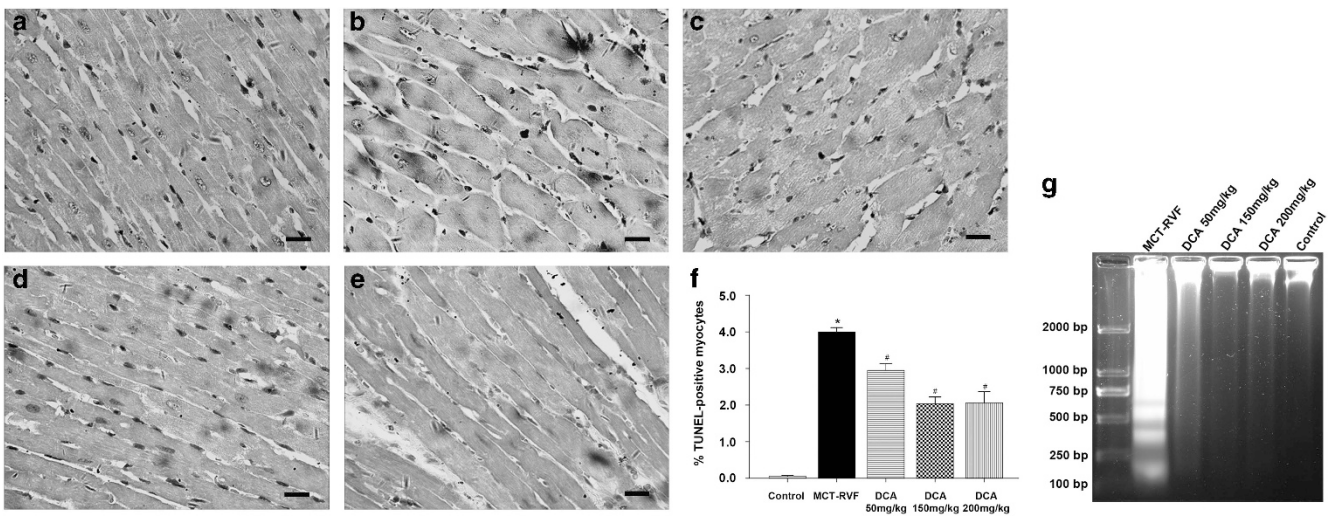

Figure 3 Dichloroacetate (DCA) inhibited myocardial apoptosis in right ventricular failure (RVF). (**a**–**e**) *In situ* detection of cardiac myocyte apoptosis was detected by terminal-deoxynucleotidyltransferase-mediated 2′-deoxyuridine 5′-triphosphated nick-end-labeling (TUNEL) assay. Compared with the control group (**a**), RV myocardial apoptosis in RVF rats was enhanced (**b**), and DCA 50 mg kg^{-1} (**c**), 150 mg kg^{-1} (**d**) and 200 mg kg^{-1} (**e**) inhibited the apoptosis; scale bar: 20 μm. (**f**) Quantitative changes in the incidence of myocardial apoptosis in RV among various treatment groups. The percentages of TUNEL-positive cells were calculated in 10 randomly chosen fields of each section at ×400 magnification. *$P<0.05$: compared with the control group; $^{\#}P<0.05$: compared with the monocrotaline-induced right ventricular failure group (MCT-RVF) group. (**g**) Representative DNA laddering of various treatment groups. DCA 50 mg kg^{-1}, DCA 50 mg kg^{-1} per day group; DCA 150 mg kg^{-1}, DCA 150 mg kg^{-1} per day group; DCA 200 mg kg^{-1}, DCA 200 mg kg^{-1} per day group. A full color version of this figure is available at the *Hypertension Research* journal online.

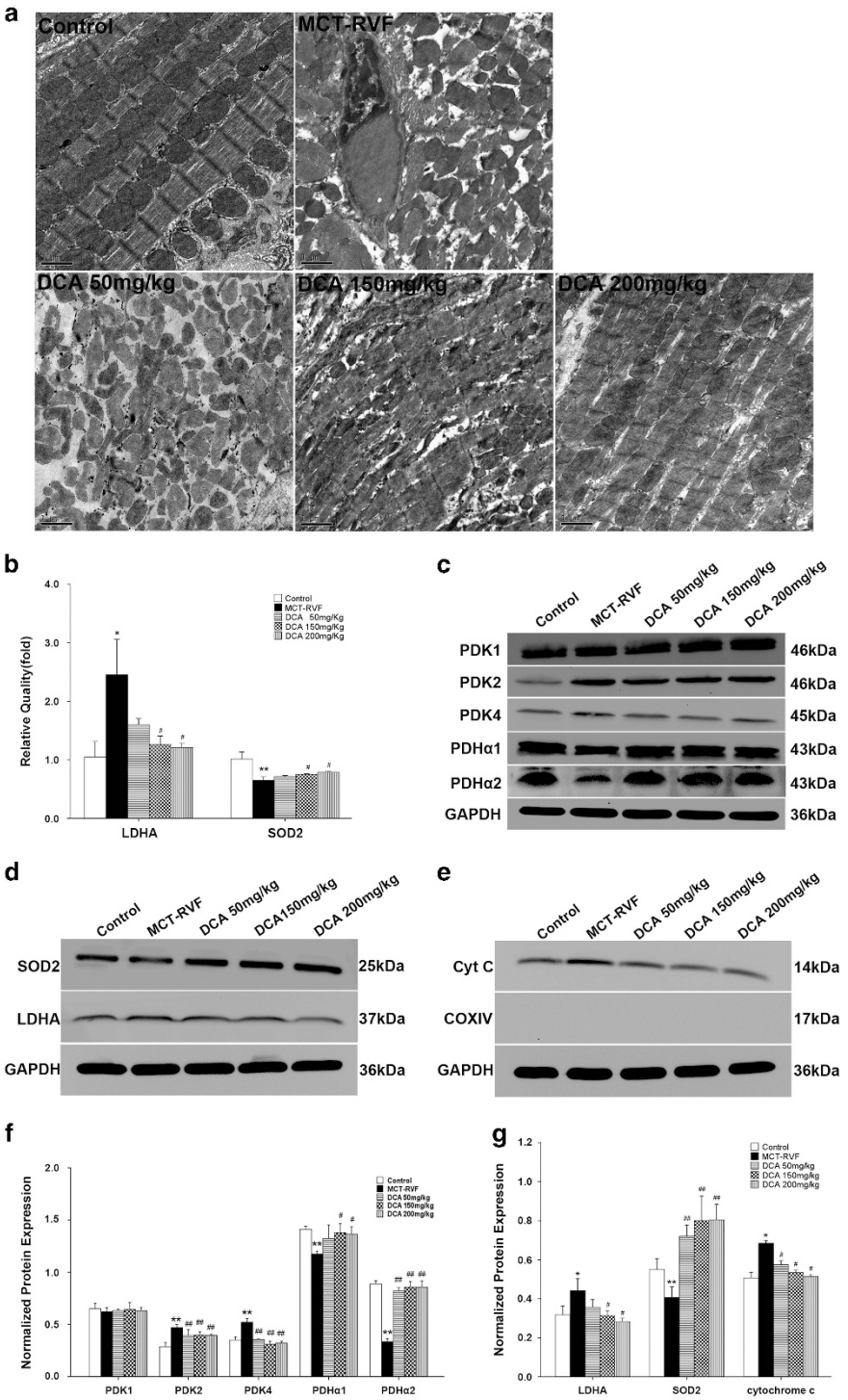

Figure 4 Dichloroacetate (DCA) restored myocardial mitochondrial function in right ventricular failure (RVF). (**a**) DCA partly reversed the abnormal mitochondrial ultrastructure in the monocrotaline-induced right ventricular failure group (MCT-RVF); scale bar = 1 μm. (**b**) Real-time polymerase chain reaction (PCR) showed that DCA inhibited the mRNA expression of lactate dehydrogenase (LDHA) and upregulated that of superoxide dismutase 2 (SOD2). (**c**) Western blots showed that increased pyruvate dehydrogenase kinase 2 and 4 (PDK2 and PDK4) expression in RV myocytes in RVF was reduced by DCA, while decreased pyruvate dehydrogenase α1 and α2 (PDHα1 and PDHα2) expression was upregulated by DCA. The expression of PDK1 was unaltered in RVF and was not influenced by DCA. (**d**) Western blots showed that DCA inhibited the protein expression of LDHA and upregulated that of SOD2. (**e**) Western blots of cytosolic fractions from various treatment groups show accumulation of cytochrome *c* (Cyt *C*) in RVF and that can be significantly suppressed by DCA. (**f** and **g**) Densitometries are shown for three rats per group, and the measurements were replicated at least three times. The gels are representative of one rat in each group from one of three separate experiments. Glyceraldehyde-3-phosphate dehydrogenase (GAPDH) in the immunoblot is shown as a loading control. $^{*}P<0.05$, $^{**}P<0.001$: compared with the control group; $^{\#}P<0.05$, $^{\#\#}P<0.001$: compared with the MCT-RVF group. COX IV, cytochrome *c* oxidase subunit IV; DCA 50 mg kg^{-1}, DCA 50 mg kg^{-1} per day group; DCA 150 mg kg^{-1}, DCA 150 mg kg^{-1} per day group; DCA 200 mg kg^{-1}, DCA 200 mg kg^{-1} per day group.

increased in the MCT-RVF group and was effectively suppressed by DCA in all three treatment groups (Figures 5a and b).

Moreover, as was shown above by cytosolic western blotting, leakage of the caspase activator cytochrome *c* from the mitochondria to the cytosol was enhanced in MCT rats. Also, DCA treatment attenuated the leakage of cytochrome *c* from the mitochondria in RV cardiomyocytes (Figures 4e and g). Caspase-9 is an initiator caspase in the mitochondrial apoptotic pathway. We measured the cleaved caspase-9 protein by western blotting. An increase in the amount of cleaved caspase-9 was observed in the MCT-RVF group, whereas treatment with DCA evidently decreased the level of caspase-9 (Figures 5a and b). Accordingly, active caspase-3 protein significantly increased in MCT-RVF rats, and DCA treatment decreased the level of this protein (Figures 5a and b). Additionally, caspase-3 activity was evidently lower in DCA-treated rats compared with MCT-RVF rats (Figure 5c). In agreement with the results of active caspase-3, poly (ADP-ribose) polymerase (PARP) cleavage increased in MCT-RVF rats, and decreased markedly in all the DCA groups (Figures 5a and b).

The effect of different DCA doses on RV was independent from changes in TPR

DCA has been reported to have effects on pulmonary vascular remodeling in MCT rats.[17] As mPAP in this study was lower with DCA treatment, it could be argued that all the RV beneficial effects of DCA were mediated by a reduction in afterload. To correct for the effects of afterload in the 50, 150 and 200 mg kg^{-1} DCA treatment groups, we calculated the correlations between TPR and the main RV parameters for the groups with different DCA doses. The effect of DCA on cytochrome *c* release from RV mitochondria did not correlate significantly with TPR (Figure 6a). Accordingly, in RVF under the treatment of DCA, no correlation was found between TPR and normalized protein expression changes of cleaved caspase-9, active caspase-3 or cleaved PARP (Figures 6b and d).

DISCUSSION

This study provides novel insight into the mechanism of mitochondria targeted therapy for PAH-induced RVF, showing that treatment with DCA is associated not only with an increased level of oxidative metabolism but also with reduced RV myocardial apoptosis and restored mitochondrial function. These findings are important because they show that a fear for increased RV myocardial apoptosis with DCA is unnecessary, as DCA promotes pulmonary arterial smooth muscle cell apoptosis in PAH. Moreover, DCA has a positive effect on hemodynamics, RV myocardial fibrosis and capillary rarefaction, metabolism and cardiac function, supporting the potential role of the drug for the treatment of PAH-induced RVF.

Although DCA is known to have benefits on RVF by regression of pulmonary vascular remodeling,[17] a recent study also suggested that DCA has direct effects on the RV by enhancing glucose oxidation and restoring RV repolarization.[9] In our study, we evaluated the effect of DCA treatment on RVF with different doses, by applying 50, 150 and 200 mg kg^{-1}. Significant differences were found in the effects of DCA between treatment groups with different doses. Although there is a potential toxicity related to a high dosage of DCA, this probably is not an issue here as no significant differences are found between the body weight of the rats in the three different groups. Besides, the dosage for long-term DCA treatment on patients with mitochondrial diseases can be 50 mg kg^{-1}, which is well tolerated. This dosage equals to about 300 mg kg^{-1} in rats, which is more than the used dosage.[24,25] To further evaluate the direct effects of DCA on RV, we calculated the correlations between the critical parameters in RV and TPR in the treatment groups with different DCA doses, and no correlation was found between TPR and the main parameters in RV including cytochrome *c* release, cleaved caspase-9, active caspase-3 and cleaved PARP protein expression. The absence of a correlation shows that there is a different DCA dose–response relationship for the effects in the lungs and for the effects in the heart, suggesting that the effects of

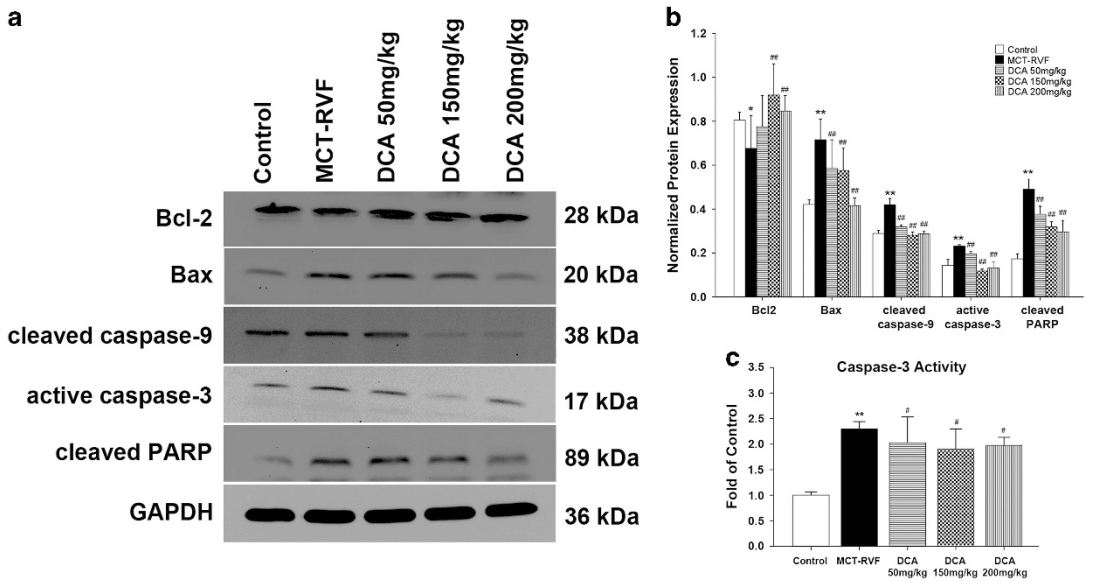

Figure 5 Dichloroacetate (DCA) regulated myocardial apoptosis in right ventricular failure (RVF) via mitochondrial apoptotic pathway. (**a** and **b**) Western blot analysis of ventricular lysates shows increased levels of BAX, cleaved caspase-9, active caspase-3, cleaved poly (ADP-ribose) polymerase (PARP) and decreased Bcl-2 in monocrotaline-induced right ventricular failure (MCT-RVF) group. DCA treatment significantly upregulated Bcl-2 levels, suppressed MCT-induced changes in the BAX levels and attenuated activation of caspases in RVF. (**c**) Caspase-3 activity increased in RVF and decreased after the treatment of DCA. Glyceraldehyde-3-phosphate dehydrogenase (GAPDH) in the immunoblot is shown as a loading control. $^{*}P<0.05$, $^{**}P<0.001$: compared with the control group; $^{\#}P<0.05$, $^{\#\#}P<0.001$: compared with the MCT-RVF group. DCA 50 mg kg^{-1}, DCA 50 mg kg^{-1} per day group; DCA 150 mg kg^{-1}, DCA 150 mg kg^{-1} per day group; DCA 200 mg kg^{-1}, DCA 200 mg kg^{-1} per day group.

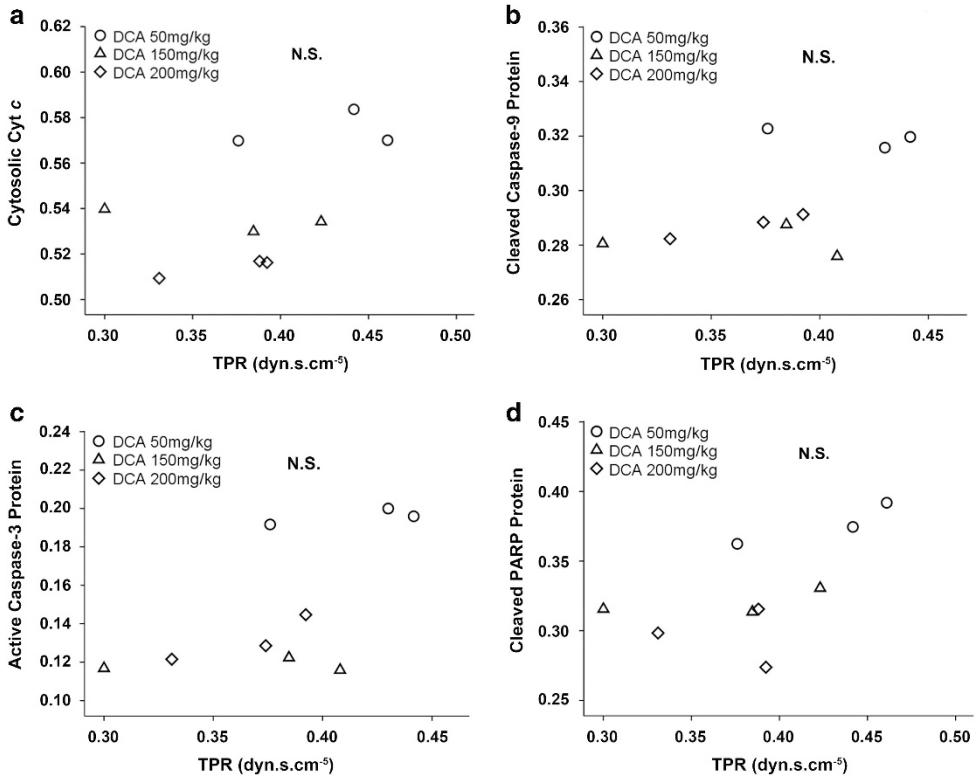

Figure 6 The effect of different dichloroacetate (DCA) doses on right ventricle (RV) was independent from changes in total pulmonary resistance (TPR). (**a**) The effect of DCA on cytochrome *c* (Cyt *c*) release from RV mitochondria did not correlate significantly with TPR. (**b**–**d**) The normalized protein expression changes of cleaved caspase-9, active caspase-3 and cleaved poly (ADP-ribose) polymerase (PARP) in RV failure (RVF) under the treatment of DCA did not correlate significantly with TPR. NS, not significant. Correlations between TPR and RV parameters were calculated using Spearman's correlation coefficients. DCA 50 mg kg^{-1}, DCA 50 mg kg^{-1} per day group; DCA 150 mg kg^{-1}, DCA 150 mg kg^{-1} per day group; DCA 200 mg kg^{-1}, DCA 200 mg kg^{-1} per day group.

DCA in the two organ systems are independent. Furthermore, we demonstrated for the first time in the MCT-RVF rat model that DCA significantly improved mitochondrial function by restoring mitochondrial structural abnormalities, reducing the cytochrome *c* release from mitochondria, upregulating the expression of SOD2 and reducing the expression of LDHA compared with untreated MCT-RVF models. Moreover, DCA reversed maladaptive RV remodeling including increased RV myocardial apoptosis and fibrosis, and decreased RV capillary density. Furthermore, we confirmed that DCA suppressed RV myocardial apoptosis by modulating the mitochondria-dependent apoptotic pathway. These results suggest that DCA has its direct benefits on RVF by improving mitochondrial function, inhibiting mitochondria-dependent apoptotic pathwayand reversing maladaptive RV remodeling.

Accumulating evidence suggests that RVF is partly attributable to metabolic derangements and mitochondrial defects.[9,10,26] The activity and expression of PDK is increased in RVF, which phosphorylates and inhibits PDH. Phosphorylated PDH inhibits formation of acetyl-CoA and slows the Krebs' cycle, causing an increase in glycolysis and a decrease in glucose oxidation.[12] In agreement with a previous study,[16] our study shows that the expression of both PDK2 and PDK4 is increased in MCT-RVF rats and that DCA significantly suppressed this expression. However, PDK1 expression was unaltered in RVF and DCA had no evident effect on it. A possible reason is that the PDK isoforms have a different transcriptional regulation. PDK1 transcription is activated by hypoxia-induced factor 1α, whereas PDK4 activation is mediated by the forkhead transcription factor (FOXO1).[9,27] Even though it has been demonstrated that the PDK activation in the lung in PAH is stimulated by redox-mediated activation of hypoxia-induced factor 1α,[28] the expression of hypoxia-induced factor 1α, mRNA or protein is unchanged in RVF while FOXO1 is found to be increased significantly,[9] which is consistent with our PDK results. Accordingly, expression of PDHα1 and PDHα2 was repressed in RVF models and was upregulated by DCA, which is in agreement with a previous study demonstrating that DCA reduced the phosphorylation of PDH.[10] Moreover, it has been recognized that deregulated metabolism contributes to the mitochondrial abnormalities,[11] which exacerbate the low oxygen condition and the abnormal metabolism.[9,10] Considering the interconnectedness of metabolism and mitochondria, we further measured the effect of DCA on mitochondrial structure by transmission electron microscopy and its effect on mitochondrial function by assessing the release of cytochrome *c* and the expression of SOD2 and LDHA. Consistent with a previous study,[10] transmission electron microscopy of the RV cardiomyocytes revealed abnormalities in the MCT-treated group that were not visible in the control group. We observed reversal of these abnormalities with DCA treatment. Moreover, the benefits of DCA on mitochondrial function were partly reflected by reduced cytochrome *c* release, reduced LDHA expression and increased SOD2 expression. LDHA is a key enzyme involved in both glycolysis and acidosis and DCA can protect mitochondria from acidosis by suppressing this enzyme. Therefore, our study for the first time suggests that DCA can attenuate mitochondrial abnormalities and improve mitochondrial function.

Mitochondria are considered to have a vital role in both cardiac remodeling and heart failure,[12,29,30] and multiple lines of evidence indicate that the progression of RVF is associated with RV remodeling, including upregulated RV myocardial apoptosis, fibrosis and decreased RV capillary density.[3] In the early stages of the disease, RV remodeling is mostly an adaptive response, but as the disease progresses, the RV dilates and RVF eventually occurs (maladaptive RV remodeling).[31] Therefore, we measured the effects of the mitochondria targeted therapy DCA on RV myocardial apoptosis by TUNEL staining and DNA laddering. RV fibrosis and capillary density were determined by Picrosirius red staining and isolectin B4 staining, respectively. Here, we show that DCA can reduce myocardial apoptosis in PAH-induced RVF *in vivo*, as confirmed by a previous *in vitro* study which suggests that DCA suppresses apoptosis in cardiomyocytes.[18] Moreover, DCA reduced fibrosis and capillary rarefaction in RV, indicating that DCA improves cardiac function and attenuates RVF partly by reversing the maladaptive RV remodeling. However, the mechanisms underlying the reverse of RV remodeling need to be further studied. It is reported that the vascular endothelial growth factor expression decreases in RVF, which could cause the capillary growth to lag behind the cardiomyocyte growth, inducing capillary rarefaction.[3] Since a recent study on neuroblastoma cells suggested that the expression of vascular endothelial growth factor could be influenced by PDK4,[32] it is reasonable to speculate that vascular endothelial growth factor may be involved in the effect of DCA on RV capillary density.

Furthermore, considering the interconnectedness of apoptosis and mitochondria,[8] here we mainly focused on the DCA regulation of myocardial apoptosis. Myocardial apoptosis has a role in RV disease progression.[4] Apoptosis is rare in the normal heart with one apoptotic cardiomyocyte in 10^4 to 10^5 cells.[33] However, apoptotic rates increase to up to 1 in 400 in human heart failure.[34,35] Apoptosis rates vary in animal models, with rates as high as 14% in ischemia/reperfusion and lower than 1% in chronic pressure overload.[36] The rate of RV myocardial apoptosis is upregulated after pulmonary artery banding in rats.[37,38] Even very low rates of apoptosis have been shown to cause lethal dilated cardiomyopathy in a mouse model.[39] It was also found that apoptotic signals can stimulate ventricular hypertrophy.[40] The Bcl-2/Bax ratio is known to determine cell apoptotic fate.[41,42] In our study, the Bcl-2/Bax ratio was reduced significantly in RV cardiomyocytes in the MCT-RVF group compared with the control group, and DCA significantly upregulated the ratio. Apoptosis detections by TUNEL and DNA laddering were consistent with the marked alterations of Bcl-2/Bax. Our study supports the hypothesis that apoptosis might be involved in a critical mechanism in the RV remodeling during the progression of pulmonary hypertension. Furthermore, we examined the expression and activity of some critical proteins related to the mitochondria-dependent apoptotic to determine the mechanisms underlying the effect of DCA on RV myocardial apoptosis. The expression of both cleaved caspase-9 and active caspase-3, as well as the activity of caspase-3, were enhanced in MCT-RVF, and were suppressed by DCA. Accordingly, PARP cleavage as the substrate of active caspase-3 increased in the MCT-RVF group, and decreased markedly in all the DCA groups. Thus, here, for the first time, we demonstrated that DCA improved cardiac function by inhibiting apoptosis in RV cardiomyocytes *in vivo* through a mechanism that involves the mitochondria-dependent pathway. This result seems to contradict the previous observation in the lung, where DCA acts to increase the mitochondria-dependent apoptosis in pulmonary arterial smooth muscle cells.[17] However, our observation is partly in agreement with another study on congestive heart failure, which shows that DCA prevents H_2O_2-induced cell apoptosis in cultured cardiomyocytes.[18] It suggests the possibility that DCA may have different effect on pulmonary arterial smooth muscle cells and RV cardiomyocytes, but the underlying mechanism needs to be further studied. In addition to Bcl-2/Bax, other upstream molecules may also be involved in the effect of DCA on myocardial apoptosis via other mechanisms. Previous studies suggest that mitochondrial reactive oxygen species increase in RVF, which oxidizes and thus activates apoptosis molecules such as p53.[43] In combination with our work, which demonstrated that DCA increased the expression of SOD2 and improved the mitochondrial function in RVF, which has a crucial role in cleaning mitochondrial reactive oxygen species,[44] DCA may possibly reduce the expression of p53 or other apoptosis molecules.

Although here we show that the cardioprotective actions of DCA are accompanied by a number of cellular and molecular changes in RVF, improved mitochondrial function and reduced RV cardiomyocyte apoptosis, more mechanistic studies are required to determine how mitochondria targeted therapy in general and DCA in particular have a direct effect on PAH-induced RVF. Our study was also limited since it only included one animal model of RVF. Direct effect of DCA on RV could be further proved by performing other animal models of RVF, such as the pulmonary artery banding rats, vascular endothelial growth factor receptor antagonist SU5416 and chronic hypoxia-induced RVF rats. In addition, there may be other possible mechanisms underlying the effect of DCA on RV apoptosis. A study on the congestive heart failure rat model suggests that DCA improves cardiac function and increases the survival of the animals by activating the pentose phosphate pathway in rat heart. Moreover, DCA decreased oxidative stress and attenuated H_2O_2-induced myocyte cell death by activating the pentose phosphate pathway.[18] Therefore, other mechanisms underlying the effects of DCA on RV remodeling are worthwhile to be further studied.

In the conclusion, our results show that DCA has a direct effect on RV and reverses maladaptive RV remodeling in RVF by suppressing RV myocardial fibrosis, increasing RV capillary density and inhibiting myocardial apoptosis via mitochondria-dependent apoptotic pathway by restoring mitochondrial functional and structural abnormalities. The present study clearly shows that a fear for increased RV myocardial apoptosis with DCA treatment is unnecessary, which provides a new theoretical basis for the use of DCA in the management of PAH and RVF in the clinic.

CONFLICT OF INTEREST

Z-CJ has acted as a consultant to and a member of scientific advisory boards for companies including Actelion, Bayer Schering, Pfizer and United Therapeutics, in addition to working as an investigator in trials involving these companies. The remaining authors declare no conflict of interest.

ACKNOWLEDGEMENTS

This work was supported by the National Natural Science Foundation of China (81170300, 81470245) and the National Science Fund for Distinguished Young Scholars (81425002). The sponsors had no involvement in the study design, data analysis, data interpretation and writing or revision of the manuscript.

Author contributions: Z-CJ, RZ and XQS designed the experiments; XQS, RZ, HDZ, PY, XJW, QHZ, LW and RJ performed the experiments and collected the data; XQS, RZ and HJB analyzed the data; XQS wrote the

manuscript and HJB revised it critically for important intellectual content; Z-CJ approved manuscript for submission.

1 Ikeda S, Satoh K, Kikuchi N, Miyata S, Suzuki K, Omura J, Shimizu T, Kobayashi K, Kobayashi K, Fukumoto Y, Sakata Y, Shimokawa H. Crucial role of Rho-kinase in pressure overload-induced right ventricular hypertrophy and dysfunction in mice. *Arterioscler Thromb Vasc Biol* 2014; **34**: 1260–1271.
2 van Wolferen SA, Marcus JT, Boonstra A, Marques KM, Bronzwaer JG, Spreeuwenberg MD, Postmus PE, Vonk-Noordegraaf A. Prognostic value of right ventricular mass, volume, and function in idiopathic pulmonary arterial hypertension. *Eur Heart J* 2007; **28**: 1250–1257.
3 Bogaard HJ, Natarajan R, Henderson SC, Long CS, Kraskauskas D, Smithson L, Ockaili R, McCord JM, Voelkel NF. Chronic pulmonary artery pressure elevation is insufficient to explain right heart failure. *Circulation* 2009; **120**: 1951–1960.
4 Campian ME, Verberne HJ, Hardziyenka M, de Bruin K, Selwaness M, van den Hoff MJ, Ruijter JM, van Eck-Smit BL, de Bakker JM, Tan HL. Serial noninvasive assessment of apoptosis during right ventricular disease progression in rats. *J Nucl Med* 2009; **50**: 1371–1377.
5 Dorn GW. Apoptotic and non-apoptotic programmed cardiomyocyte death in ventricular remodelling. *Cardiovasc Res* 2008; **81**: 465–473.
6 Zuo XR, Wang Q, Cao Q, Yu YZ, Wang H, Bi LQ, Xie WP, Wang H. Nicorandil prevents right ventricular remodeling by inhibiting apoptosis and lowering pressure overload in rats with pulmonary arterial hypertension. *PLoS ONE* 2012; **7**: e44485.
7 Bogaard HJ, Natarajan R, Mizuno S, Abbate A, Chang PJ, Chau VQ, Hoke NN, Kraskauskas D, Kasper M, Salloum FN, Voelkel NF. Adrenergic receptor blockade reverses right heart remodeling and dysfunction in pulmonary hypertensive rats. *Am J Respir Cirt Care Med* 2010; **182**: 652–660.
8 Adrain C, Martin SJ. The mitochondrial apoptosome: a killer unleashed by the cytochrome seas. *Trends Biochem Sci* 2001; **26**: 390–397.
9 Piao L, Sidhu VK, Fang YH, Ryan JJ, Parikh KS, Hong Z, Toth PT, Morrow E, Kutty S, Lopaschuk GD, Archer SL. FOXO1-mediated upregulation of pyruvate dehydrogenase kinase-4 (PDK4) decreases glucose oxidation and impairs right ventricular function in pulmonary hypertension: therapeutic benefits of dichloroacetate. *J Mol Med (Berl)* 2013; **91**: 333–346.
10 Piao L, Fang YH, Cadete VJ, Wietholt C, Urboniene D, Toth PT, Marsboom G, Zhang HJ, Haber I, Rehman J, Lopaschuk GD, Archer SL. The inhibition of pyruvate dehydrogenase kinase improves impaired cardiac function and electrical remodeling in two models of right ventricular hypertrophy: resuscitating the hibernating right ventricle. *J Mol Med (Berl)* 2010; **88**: 47–60.
11 Gomez-Arroyo J, Mizuno S, Szczepanek K, Van Tassell B, Natarajan R, dos Remedios CG, Drake JI, Farkas L, Kraskauskas D, Wijesinghe DS, Chalfant CE, Bigbee J, Abbate A, Lesnefsky EJ, Bogaard HJ, Voelkel NF. Metabolic gene remodeling and mitochondrial dysfunction in failing right ventricular hypertrophy due to pulmonary arterial hypertension. *Circ Heart Fail* 2013; **6**: 136–144.
12 Sugden MC, Langdown ML, Harris RA, Holness MJ. Expression and regulation of pyruvate dehydrogenase kinase isoforms in the developing rat heart and in adulthood: role of thyroid hormone status and lipid supply. *Biochem J* 2000; **352**: 731–738.
13 Neubauer S. The failing heart—an engine out of fuel. *N Engl J Med* 2007; **356**: 1140–1151.
14 Stacpoole PW. The pharmacology of dichloroacetate. *Metabolism* 1989; **38**: 1124–1144.
15 Piao L, Marsboom G, Archer SL. Mitochondrial metabolic adaptation in right ventricular hypertrophy and failure. *J Mol Med (Berl)* 2010; **88**: 1011–1020.
16 Finck BN, Kelly DP. PGC-1 coactivators: inducible regulators of energy metabolism in health and disease. *J Clin Invest* 2006; **116**: 615–622.
17 McMurtry MS, Bonnet S, Wu X, Dyck JR, Haromy A, Hashimoto K, Michelakis ED. Dichloroacetate prevents and reverses pulmonary hypertension by inducing pulmonary artery smooth muscle cell apoptosis. *Circ Res* 2004; **95**: 830–840.
18 Kato T, Niizuma S, Inuzuka Y, Kawashima T, Okuda J, Tamaki Y, Iwanaga Y, Narazaki M, Matsuda T, Soga T, Kita T, Kimura T, Shioi T. Analysis of metabolic remodeling in compensated left ventricular hypertrophy and heart failure. *Circ Heart Fail* 2010; **3**: 420–430.
19 Guo Q, Huang JA, Yamamura A, Yamamura H, Zimnicka AM, Fernandez R, Yuan JX. Inhibition of the Ca(2+)-sensing receptor rescues pulmonary hypertension in rats and mice. *Hypertens Res* 2014; **37**: 116–124.
20 Cowan KN, Heilbut A, Humpl T, Lam C, Ito S, Rabinovitch M. Complete reversal of fatal pulmonary hypertension in rats by a serine elastase inhibitor. *Nat Med* 2000; **6**: 698–702.
21 Ricke-Hoch M, Bultmann I, Stapel B, Condorelli G, Rinas U, Sliwa K, Scherr M, Hilfiker-Kleiner D. Opposing roles of Akt and STAT3 in the protection of the maternal heart from peripartum stress. *Cardiovasc Res* 2014; **101**: 587–596.
22 Li J, Zhang DS, Ye JC, Li CM, Qi M, Liang DD, Xu XR, Xu L, Liu Y, Zhang H, Zhang YY, Deng FF, Feng J, Shi D, Chen JJ, Li L, Chen G, Sun YF, Peng LY, Chen YH. Dynamin-2 mediates heart failure by modulating Ca^{2+}-dependent cardiomyocyte apoptosis. *Int J Cardiol* 2013; **168**: 2109–2119.
23 Sinha-Hikim I, Shen R, Nzenwa I, Gelfand R, Mahata SK, Sinha-Hikim AP. Minocycline suppresses oxidative stress and attenuates fetal cardiac myocyte apoptosis triggered by *in utero* cocaine exposure. *Apoptosis* 2011; **16**: 563–573.
24 Barshop BA, Naviaux RK, McGowan KA, Levine F, Nyhan WL, Loupis-Geller A, Haas RH. Chronic treatment of mitochondrial disease patients with dichloroacetate. *Mol Genet Metab* 2004; **83**: 138–149.
25 Reagan-Shaw S, Nihal M, Ahmad N. Dose translation from animal to human studies revisited. *FASEB J* 2008; **22**: 659–661.
26 Fang YH, Piao L, Hong Z, Toth PT, Marsboom G, Bache-Wiig P, Rehman J, Archer SL. Therapeutic inhibition of fatty acid oxidation in right ventricular hypertrophy: exploiting Randle's cycle. *J Mol Med (Berl)* 2012; **90**: 31–43.
27 Kim JW, Tchernyshyov I, Semenza GL, Dang CV. HIF-1-mediated expression of pyruvate dehydrogenase kinase: a metabolic switch required for cellular adaptation to hypoxia. *Cell Metab* 2006; **3**: 177–185.
28 Marsboom G, Wietholt C, Haney CR, Toth PT, Ryan JJ, Morrow E, Thenappan T, Bache-Wiig P, Piao L, Paul J, Chen CT, Archer SL. Lung (1)(8)F-fluorodeoxyglucose positron emission tomography for diagnosis and monitoring of pulmonary arterial hypertension. *Am J Respir Crit Care Med* 2012; **185**: 670–679.
29 Tsutsui H, Kinugawa S, Matsushima S. Mitochondrial oxidative stressand dysfunction in myocardial remodelling. *Cardiovasc Res* 2009; **81**: 449–456.
30 Rodrigues JQ, da Silva ED Jr, de Magalhães Galvão K, Miranda-Ferreira R, Caricati-Neto A, Jurkiewicz NH, Garcia AG, Jurkiewicz A. Differential regulation of atrial contraction by P1 and P2 purinoceptors in normotensive and spontaneously hypertensive rats. *Hypertens Res* 2014; **37**: 210–219.
31 Haddad F, Ashley E, Michelakis ED. New insights for the diagnosis and management of right ventricular failure, from molecular imaging to targeted right ventricular therapy. *Curr Opin Cardiol* 2010; **25**: 131–140.
32 Rellinger EJ, Romain C, Choi S, Qiao J, Chung DH. Silencing gastrin-releasing peptide receptor suppresses key regulators of aerobic glycolysis in neuroblastoma cells. *Pediatr Blood Cancer* 2015; **62**: 581–586.
33 Soonpaa MH, Field LJ. Survey of studies examining mammalian cardiomyocyte DNA synthesis. *Circ Res* 1998; **83**: 15–26.
34 Hein S, Arnon E, Kostin S, Schönburg M, Elsässer A, Polyakova V, Bauer EP, Klövekorn WP, Schaper J. Progression from compensated hypertrophy to failure in the pressure-overloaded human heart: structural deterioration and compensatory mechanisms. *Circulation* 2003; **107**: 984–991.
35 Olivetti G, Abbi R, Quaini F, Kajstura J, Cheng W, Nitahara JA, Quaini E, Di Loreto C, Beltrami CA, Krajewski S, Reed JC, Anversa P. Apoptosis in the failing human heart. *N Engl J Med* 1997; **336**: 1131–1141.
36 Kang PM, Izumo S. Apoptosis and heart failure: a critical review of the literature. *Circ Res* 2000; **86**: 1107–1113.
37 Ikeda S, Hamada M, Hiwada K. Cardiomyocyte apoptosis with enhanced expression of P53 and Bax in right ventricle after pulmonary arterial banding. *Life Sci* 1999; **65**: 925–933.
38 Braun MU, Szalai P, Strasser RH, Borst MM. Right ventricular hypertrophy and apoptosis after pulmonary artery banding: regulation of PKC isozymes. *Cardiovasc Res* 2003; **59**: 658–667.
39 Wencker D, Chandra M, Nguyen K, Miao W, Garantziotis S, Factor SM, Shirani J, Armstrong RC, Kitsis RN. A mechanistic role for cardiac myocyte apoptosis in heart failure. *J Clin Invest* 2003; **111**: 1497–1504.
40 Hirotani S, Otsu K, Nishida K, Higuchi Y, Morita T, Nakayama H, Yamaguchi O, Mano T, Matsumura Y, Ueno H, Tada M, Hori M. Involvement of nuclear factor-kappaB and apoptosis signal-regulating kinase 1 in G-protein-coupled receptor agonist-induced cardiomyocyte hypertrophy. *Circulation* 2002; **105**: 509–515.
41 Gross A. BCL-2 proteins: regulators of the mitochondrial apoptotic program. *IUBMB Life* 2001; **52**: 231–236.
42 Adams JM, Cory S. The Bcl-2 protein family: arbiters of cell survival. *Science* 1998; **281**: 1322–1326.
43 Liu B, Chen Y, Clair. DK St. ROS and p53: a versatile partnership. *Free Radic Biol Med* 2008; **44**: 1529–1535.
44 Pias EK, Ekshyyan OY, Rhoads CA, Fuseler J, Harrison L, Aw TY. Differential effects of superoxide dismutase isoform expression on hydroperoxide-induced apoptosis in PC-12 cells. *J Biol Chem* 2003; **278**: 13294–13301.